Crossover and thermodynamic representation in the extended η model for fractal growth

Takashi Nagatani
College of Engineering, Shizuoka University, Hamamatsu 432, Japan
and Center for Polymer Studies, Boston University, Boston, Massachusetts 02215

H. Eugene Stanley
Center for Polymer Studies, Boston University, Boston, Massachusetts 02215
(Received 11 May 1990)

The η model for the dielectric breakdown is extended to the case where double power laws apply. It is shown that a crossover phenomenon between the diffusion-limited aggregation (DLA) fractal and the η fractal occurs in the extended η model. Through the use of the dimensional analysis, a dimensionless parameter is found to govern the crossover. It is shown that when $\eta < 1$ the crossover from the DLA fractal to the η fractal occurs with increasing size, and if $\eta > 1$ the inverse crossover from the η fractal to the DLA fractal appears. It is also shown that the crossover radius is controlled by changing the applied field. The global flow diagram in the two-parameter space is obtained by using a two-parameter position-space renormalization-group approach. The crossover exponent and the crossover radius are calculated. The crossover phenomenon is described in terms of a thermodynamic representation of the two-phase equilibrium.

I. INTRODUCTION

Fractal growth phenomena in pattern formation have recently attracted considerable attention.[1-10] Patterns forming in diffusive systems all give rise to similar structures to the diffusion-limited aggregation (DLA) fractal at specific conditions. Examples of pattern formation in diffusive systems include viscous fingering, electrochemical deposition, crystal growth, and dielectric breakdown. An approximation to these phenomena is provided by the Laplacian growth model. The growth probability on the interface of a pattern is determined by the harmonic measure, which is proportional to the current on the interface. Niemeyer, Pietronero, and Wiesmann have proposed an extended DLA model for the dielectric breakdown. The model is called the η model.[11] The growth probability p_i at the point i on the interface is given by

$$p_i = \frac{E_i^\eta}{\sum_i E_i^\eta} , \tag{1}$$

where E_i is the electric field at the point i on the interface $E_i = -\nabla\Phi$ and Φ is the electrostatic potential satisfying the Laplace equation. The fractal dimension of the pattern formed in the dielectric breakdown model decreases from 2 (dense pattern) to 1 (needle pattern) with increasing η. For $\eta = 1$ the resulting pattern becomes the DLA fractal.[12]

In real experimental situations, a variety of crossover phenomena appear. For example, Grier *et al.*[13] found the crossover from the DLA fractal, through the dense structure, to the dendrite in the electrodeposition experiment. Lenormand[14] found that by tuning the flow rate in porous media made of interconnected channels, the pattern of the injected fluid evolves continuously from invasion percolation to DLA. In computer simulations, some crossovers were also found from the DLA fractal to the dense structure or from the dense structure to the DLA fractal.[15-17]

Very recently, Lee, Coniglio, and Stanley[18] succeeded in analyzing the crossover from the DLA fractal to the dense structure in viscous fingering at a finite viscosity ratio. They extended the position-space renormalization-group method devised by Nagatani[19] and developed a two-parameter renormalization-group method to study the crossover. They showed the global flow diagram in the two-parameter space and calculated the crossover exponent and the crossover radius. Nagatani[20] also succeeded in analyzing the effect of the sticking probability on DLA by using the two-parameter position-space renormalization-group method. It was found that when the sticking probability was small the aggregate had to cross over from the dense structure to the DLA fractal. The crossover was consistent with the simulation by Meakin.[21]

In this paper, we propose an extended η model to show crossover phenomena. We extend the η model to the case where double power laws apply. The growth velocity in the normal direction on the interface is given by

$$v_n \approx \sigma \frac{\partial\Phi}{\partial n} + \sigma_\eta \left(\frac{\partial\Phi}{\partial n} \right)^\eta , \tag{2}$$

where Φ is the electrostatic potential satisfying the Laplace equation and $\partial\Phi/\partial n$ is the derivative normal to the interface. The growth rate in this model is controlled by two powers: 1 and η. In the limiting case of $\sigma \gg \sigma_\eta$, the growth rule (2) reduces to the DLA model. The pattern becomes the DLA fractal. On the other hand, in the limiting case of $\sigma \ll \sigma_\eta$, the growth rule (2) reduces to the η model. The pattern becomes the η fractal determined by

the η power. In this model one can expect that a crossover phenomenon occurs between the DLA fractal and the η fractal. We investigate the crossover phenomena by using dimensional analysis and the two-parameter position-space renormalization-group method. We show that the crossover phenomena are described in terms of a thermodynamic representation of the two-phase equilibrium.

The organization of the paper is as follows. In Sec. II we present the dimensional analysis to describe the crossover qualitatively. In Sec. III we apply the two-parameter position-space renormalization-group method to the extended η model on the hierarchical diamond lattice. We show the global flow diagram in two-parameter space. In Sec. IV we describe the crossover phenomena in terms of a thermodynamic representation of an equilibrium state of the two phases. In Sec. V we present the summary.

II. MODEL AND DIMENSIONAL ANALYSIS

We extend the η model to the case with the two powers. We consider a dielectric breakdown problem. The electrostatic potential satisfies the Laplace equation

$$\nabla^2\Phi=0 . \tag{3}$$

The boundary conditions on the interface and at far field are given by the constant voltages

$$\Phi=\begin{cases}0 \text{ on the interface}\\ \Phi_0 \text{ at far field} .\end{cases} \tag{4}$$

Here Φ_0 represents the applied voltage. The growth velocity of the interface is assumed to be given by the growth rule (2). The η model is extended to the case with two power laws. We study the crossover between the DLA fractal and the η fractal by using the dimensional analysis. We can conjecture the crossover qualitatively without solving the Laplace equation. For many electric systems one can select a characteristic length and a characteristic electrostatic potential. Thus the characteristic length is usually taken to be the pattern size L and the characteristic electrostatic potential Φ_0. Once this choice has been made, we may define the following dimensionless variables and differential operations:

$$\begin{aligned} &x^*=x/L,\quad y^*=y/L ;\\ &\Phi^*=\Phi/\Phi_0,\quad \nabla^*=L\nabla .\end{aligned} \tag{5}$$

We rewrite the Laplace equation (3) with the boundary conditions (4) and the growth rule (2) in terms of the foregoing dimensionless variables

$$\nabla^{*2}\Phi^*=0 , \tag{3'}$$

$$\Phi^*=\begin{cases}0 \text{ on the interface}\\ 1 \text{ at far field} ,\end{cases} \tag{4'}$$

and

$$v_n^*\approx(\nabla^*\Phi^*)+\chi(\nabla^*\Phi^*)^\eta \tag{2'}$$

with

$$\chi=\sigma_\eta\Phi_0^{\eta-1}/\sigma L^{\eta-1} . \tag{6}$$

Note that in the dimensionless form the "scale factors," that is, those variables describing the overall size and the applied voltage are concentrated in one dimensionless group χ. If χ is sufficiently small, the growth rule (2') reduces to the DLA model. On the other hand, when χ is sufficiently large, the growth rule (2') reduces to the η model. The dimensionless parameter χ governs the crossover between the DLA fractal and the η factal. If $\eta<1$, the dimensionless parameter χ becomes larger and larger with increasing length L. Also χ becomes smaller and smaller with increasing applied voltage. The crossover from the DLA fractal to the η fractal occurs with increasing size. The crossover is controlled by changing the applied voltage. With increasing applied voltage, the DLA fractal part increases and the η fractal part decreases. If $\eta>1$, the crossover between the DLA fractal and the η fractal is inverted. The crossover from the η fractal to the DLA fractal occurs with increasing size. With decreasing applied voltage, the η fractal part decreases and the DLA fractal part increases. We note that this model has the characteristic property that the crossover radius depends on the applied voltage. The crossover radius between the DLA fractal and the η fractal can be controlled by changing the applied voltage.

In order to quantify this crossover behavior, we define a crossover exponent ϕ and a crossover radius r_c. We propose the scaling ansatz

$$M(r,\chi)=\begin{cases}r^{d_f}F(\chi r^\phi) & \text{if } \eta<1 \qquad (7)\\ r^{d_\eta}F'(\chi^{-1}r^\phi) & \text{if } \eta>1 \qquad (7')\end{cases}$$

where M is the mass of the cluster, r the radius of gyration, d_f the fractal dimension of the DLA fractal, d_η the fractal dimension of the η fractal, and $\chi=\sigma_\eta\Phi_0^{\eta-1}/\sigma L^{\eta-1}$. The scaling functions are assumed as follows:

$$F(x)\approx\begin{cases}1 & \text{if } x\ll 1\\ x^{(d_\eta-d_f)/\phi} & \text{if } x\gg 1 ,\end{cases} \tag{8}$$

$$F'(x)\approx\begin{cases}1 & \text{if } x\ll 1\\ x^{(d_f-d_\eta)/\phi} & \text{if } x\gg 1 .\end{cases} \tag{8'}$$

The crossover radius scales as $r_c\approx\chi^{-1/\phi}(\eta<1)$ and $r_c\approx\chi^{1/\phi}(\eta>1)$. Explicitly the crossover radius scales as follows:

$$r_c\approx\begin{cases}\Phi_0^{(1-\eta)/\phi} & (\eta<1)\\ \Phi_0^{(\eta-1)/\phi} & (\eta>1)\end{cases} \tag{9}$$

at constant length,

$$r_c\approx\begin{cases}L^{-(1-\eta)/\phi} & (\eta<1)\\ L^{-(\eta-1)/\phi} & (\eta>1)\end{cases} \tag{10}$$

at constant voltage. We cannot obtain the crossover exponent ϕ by using dimensional analysis. The crossover exponent is obtained by using the two-parameter position-space renormalization-group method. Our scal-

ing ansatz has a characteristic property depending upon the applied voltage Φ_0 through χ.

III. RENORMALIZATION-GROUP APPROACH

We analyze the crossover between the DLA fractal and the η fractal by using the two-parameter position-space renormalization-group method. For simplicity, we consider the dielectric breakdown problem on the diamond hierarchical lattice. The position-space renormalization-group approach to the hierarchical lattice is comparatively accurate to derive the critical behavior of the system. The diamond hierarchical lattice is constructed by an iterative generation of the base set. Each bond is occupied by the resistor of unit conductance. A constant voltage is applied between the bottom and the top on the diamond hierarchical lattice. The dielectric breakdown proceeds from the bottom to the top. Figure 1 shows the illustration of the breakdown model on the diamond lattice. The thick lines indicate breakdown bonds which construct the breakdown pattern. The bonds on the perimeter of the breakdown pattern are represented by the wavy lines. The thin lines indicate unbroken bonds, which are resistors of unit conductance. The resistor network problem is solved under the boundary conditions of the constant applied voltage. A growth probability is assigned to the perimeter bond following the growth rule (2). The growth probability p_i at the growth-perimeter bond i is given by

$$p_i=(\sigma V_i+\sigma_\eta V_i^\eta)\Big/\left[\sum_i(\sigma V_i+\sigma_\eta V_i^\eta)\right], \tag{11}$$

where V_i is the voltage on the perimeter bond i. The breakdown occurs on the perimeter bond according to the growth probability. The interface proceeds to the top just after breaking down. The breakdown process of bonds is assumed to occur one by one.

We consider the renormalization procedure for deriving the two-parameter position-space renormalization-group equations. We derive the renormalization transformations for the linear conductance σ and the nonlinear conductance σ_η of the perimeter bond. We will show that the two-parameter renormalization-group equations are given by

$$\sigma'=R_1(\sigma,\sigma_\eta)\ , \tag{12}$$

$$\sigma'_\eta=R_\eta(\sigma,\sigma_\eta)\ . \tag{13}$$

We distinguish between three types of bonds on the lattice before and after a renormalization procedure: (a) breakdown bonds that are occupied by superconducting bonds and construct the breakdown pattern, (b) growth bonds that are on the surface of the breakdown pattern and can be successively grown, and (c) unbroken bonds that construct the electric field in the exterior of the breakdown pattern and are not the growth bond. The breakdown, growth, and unbroken bonds are respectively indicated by the thick, wavy, and thin lines in the figures. We partition all the space of the diamond hierarchical lattice into cells of size $b=2$ (b is the scale factor), each containing a single generator. After a renormalization transformation these cells play the role of "renormalized" bonds. The nth generation of the hierarchical lattice is transformed to the $(n-1)$th generation. The renormalized bonds are then classified into the three types of bonds, similarly to bonds before the renormalization. If a cell is spanned with the bonds occupied by the breakdown bond, then the cell is renormalized as a breakdown bond. If the cell is not spanned with the breakdown bond and is nearest neighbor to the breakdown pattern, then the cell is renormalized as the growth bond on the interface. When the cell is constructed only by unbroken bonds and is not nearest neighbor to the breakdown pattern, then the cell is renormalized as an unbroken bond. Since the resistor-network problem is the discrete version of the Laplace equation, the voltage at each node is given by solving the linear resistor network. The linear conductance of the breakdown bond remains an infinite value after renormalization. The linear conductance of the unbroken bond after renormalization also remains a unit value. The linear and nonlinear conductances of the growth bond are respectively transformed to different values after renormalization. We shall derive the renormalization transformations of the linear and nonlinear conductances. We assume that breakdown process occurs stepwise: the breakdown proceeds one by one, and only one bond breaks at a time (there is no simultaneous bond breaking). Figure 2 shows all the configurations of the cell for which it is possible to renormalize as the growth bond. Let us consider the configurational probability C_α with which a particular configuration α appears. The distinct configurations are labeled by α ($\alpha=a,b,c$) on the left-hand side in Fig. 2. Each cell on the left-hand side is renormalized to the growth bond on the right-hand side. The configuration (b) is constructed by adding a breakdown bond onto the growth bonds 1 or 2 in the configuration (a). The probability with which a breakdown bond adds onto the growth bonds 1 or 2 in the configuration (a) is given by the growth probabilities

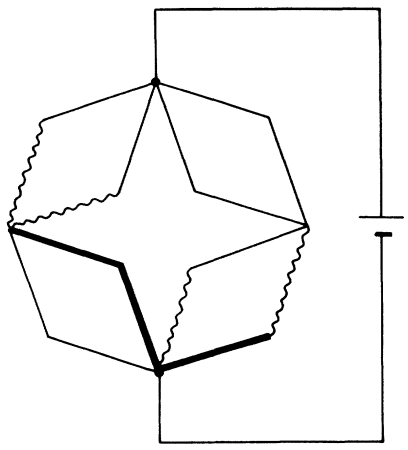

FIG. 1. Illustration of the dielectric breakdown model on the diamond hierarchical lattice. A constant voltage is applied between the top and the bottom. The thick, wavy, and thin lines indicate, respectively, breakdown, growth, and unbroken bonds.

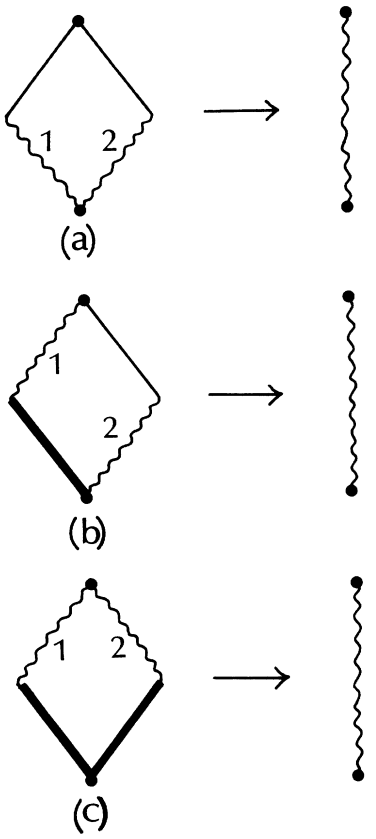

FIG. 2. All distinct configurations (a), (b), and (c) of the cell that are possible to renormalize as the growth bond. Each cell on the left-hand side is renormalized to the growth bond on the right-hand side.

$p_{a,1}$ or $p_{a,2}$ of the growth bonds 1 or 2 in the configuration (a). In addition, by adding a breakdown bond to the configuration (b), the configuration (c) occurs. The configurational probabilities C_α are given by

$$C_b = C_a(p_{a,1}+p_{a,2}), \quad C_c = C_b p_{b,2} , \tag{14}$$

where $p_{a,1}=p_{a,2}=\frac{1}{2}$. The configurational probability C_a is determined from the normalization condition

$$\sum_\alpha C_\alpha = C_a + C_b + C_c = 1 . \tag{15}$$

The voltages on the nodes within the cells are determined by the linear-resistor-network problem. Consider the resistor-network problem for each cell that can be renormalized as a growth bond. We apply the constant voltage V between the top and the bottom for each cell. We solve the linear resistor network to obtain the voltage at each node. The currents $I_{\alpha,i}$ flowing on the growth bonds of each cell are given by

$$\begin{aligned} &I_{a,1}=I_{a,2}=[\sigma/(1+\sigma)]V , \\ &I_{b,1}=\sigma V, \quad I_{b,2}=[\sigma/(1+\sigma)]V , \\ &I_{c,1}=I_{c,2}=\sigma V . \end{aligned} \tag{16}$$

By using the above relations (16), the renormalized growth velocities v'_α for each cell are obtained

$$\begin{aligned} v'_a &\approx [2\sigma/(1+\sigma)]V + 2\sigma_\eta(1+\sigma)^{-\eta}V^\eta , \\ v'_b &\approx [\sigma+\sigma/(1+\sigma)]V + \sigma_\eta[1+(1+\sigma)^{-\eta}]V^\eta , \\ v'_c &\approx 2\sigma V + 2\sigma_\eta V^\eta . \end{aligned} \tag{17}$$

The renormalized linear conductances and the renormalized nonlinear conductances for the cells are given by

$$\begin{aligned} &\sigma'_a = 2\sigma/(1+\sigma), \quad \sigma'_{\eta,a} = 2\sigma_\eta(1+\sigma)^{-\eta} , \\ &\sigma'_b = \sigma+\sigma/(1+\sigma), \quad \sigma'_{\eta,b} = \sigma_\eta[1+(1+\sigma)^{-\eta}] , \\ &\sigma'_c = 2\sigma, \quad \sigma'_{\eta,c} = 2\sigma_\eta . \end{aligned} \tag{18}$$

The linear conductances of each cell agree with those of the ordinary DLA. The growth probabilities $p_{\alpha,i}$ within the cell α are given by

$$\begin{aligned} &p_{a,1}=p_{a,2}=\tfrac{1}{2} , \\ &p_{b,1}=(\sigma+\sigma_\eta)/[\sigma+\sigma/(1+\sigma)+\sigma_\eta+\sigma_\eta(1+\sigma)^{-\eta}] , \\ &p_{b,2}=1-p_{b,1} , \\ &p_{c,1}=p_{c,2}=\tfrac{1}{2} . \end{aligned} \tag{19}$$

When the nonlinear conductance equals zero, the growth probabilities are consistent with the ordinary DLA. The renormalized linear conductance and the renormalized nonlinear conductance of the growth bond will be assumed to be given by the most probable values

$$\sigma' = \exp\left[\sum_\alpha C_\alpha \ln\sigma'_\alpha\right] , \tag{20}$$

$$\sigma'_\eta = \exp\left[\sum_\alpha C_\alpha \ln\sigma'_{\eta,\alpha}\right] . \tag{21}$$

The relationships (20) and (21) with (14), (15), (18), and (19) present the renormalization-group equations (12) and (13). Equations (14), (15), and (18)–(21) are simultaneously solved. We find the two nontrivial fixed points ($\sigma^*=2.123$, $\sigma^*_\eta=0$) and ($\sigma^*=c$, $\sigma^*_\eta=\infty$) where c is a constant depending upon the parameter η. The fixed point ($\sigma^*=2.123$, $\sigma^*_\eta=0$) gives the ordinary DLA. It is called the DLA point. On the other hand, the fixed point ($\sigma^*=c$, $\sigma^*_\eta=\infty$) gives the η model. It is called the η point. We study the stability of the fixed point. We obtain the global flow diagram in the two-parameter space. We transform the parameter σ_η to the following:

$$A = \sigma_\eta/(1+\sigma_\eta) . \tag{22}$$

We consider the crossover phenomena between the DLA fractal and the η fractal. To find the global flow diagram in the two-parameter space (σ, A), we randomly choose a point in the parameter space (σ, A) and calculate the renormalized linear conductance and the renormalized nonlinear conductance using (20) and (21) to find a new point (σ', A'). We repeat this process to find next point (σ'', A''), and continue until we approach a stable fixed point. We use some initial points and plot the renormalization flow in the phase space for representative

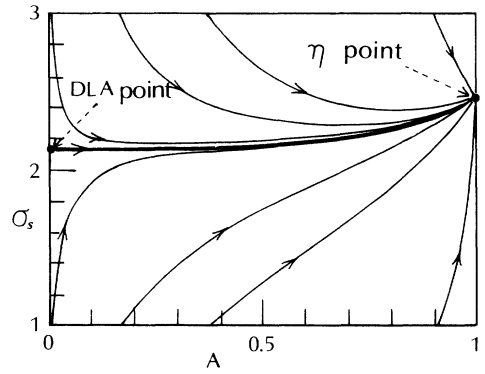

FIG. 3. Global flow diagram in two-parameter space (σ_s, A) for $\eta=0.2$. There are two fixed points: the DLA point and the η point. All the renormalization flows eventually merge into the η point. The crossover occurs from the DLA fractal to the η fractal. The crossover line from the DLA fractal to the η fractal is indicated by the thick line.

initial points. Figures 3–5 show the global flow diagrams for $\eta=0.2$, 2, and 4. From the renormalization flow, we can determine the stabilities of the two fixed points: the DLA point and the η point. First, we consider the case of $\eta=0.2$. The DLA point is a saddle point. The η point is stable in every direction. All the renormalization flows eventually merge into the η point. It is found from the flow diagram that there exists a crossover from the DLA fractal to the dense η fractal. The crossover line can be determined by following the renormalization flow, which starts from an initial point very close to the DLA point. It is indicated by the thick line in Fig. 3. Second, we consider the cases of $\eta=2$ and 4. The η point is a saddle point. The DLA point is stable in every direction. All the renormalization flows eventually merge into the DLA point. It is found that there exists a crossover from the lean η fractal to the DLA fractal. The direction of the crossover for $\eta>1$ is inverse to that for $\eta<1$. We show the structures of the breakdown pattern for $\eta<1$ and $\eta>1$ in Figs. 6(a) and 6(b). We consider the breakdown

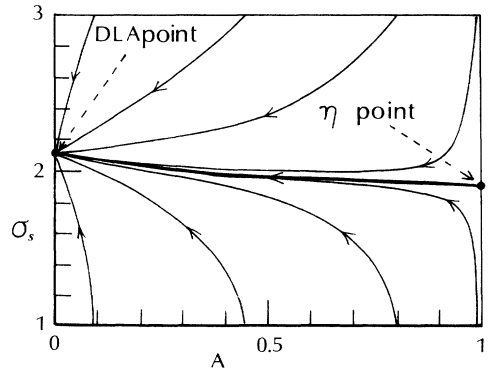

FIG. 4. Global flow diagram for $\eta=2$. There are two fixed points: the DLA point and the η point. All the renormalization flows eventually merge into the DLA point. The crossover occurs from the η fractal to the DLA fractal.

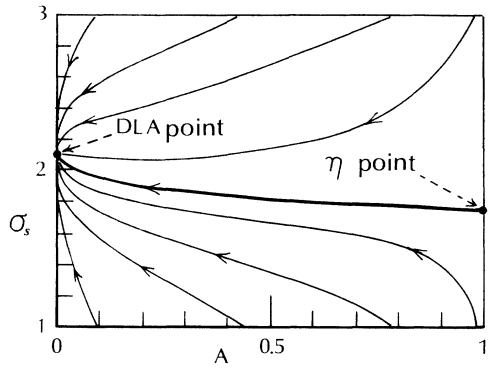

FIG. 5. Global flow diagram for $\eta=4$. All the renormalization flows eventually merge into the DLA point. The crossover occurs from the η fractal to the DLA fractal.

pattern starting from a single seed. For $\eta<1$, the inside structure of the breakdown pattern is the DLA fractal, and the outside structure the dense η fractal. For $\eta>1$, the inside structure of the pattern is the lean η fractal and

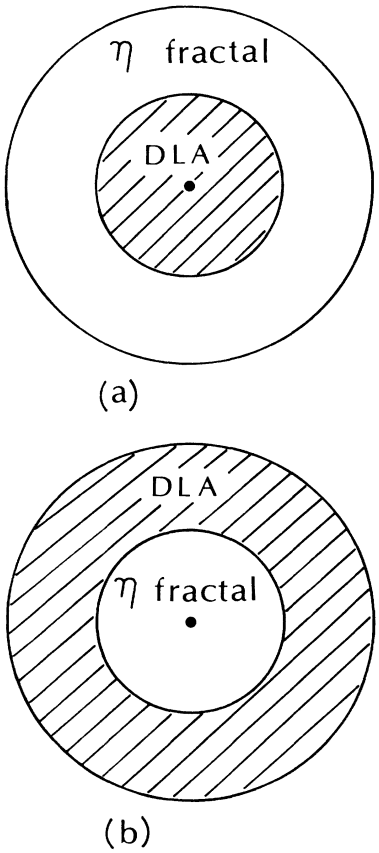

FIG. 6. Illustration of the breakdown structures. (a) The structure of the breakdown pattern for $\eta<1$. The inside structure of the breakdown pattern is the DLA fractal, and the outside structure the dense η fractal. The part of the DLA fractal increases with increasing applied voltage. (b) The structure of the breakdown pattern for $\eta>1$. The inside structure of the pattern is the lean η fractal, and the outside structure the DLA fractal. The part of the lean η fractal increases with increasing applied voltage.

the outside structure the DLA fractal.

We shall derive the crossover exponent ϕ. The crossover radius scales as $r_c \approx \sigma_\eta^{-1/\phi}$ $(\eta<1)$ and $r_c \approx (1/\sigma_\eta)^{-1/\phi}$ $(\eta>1)$. The crossover exponent can be found by linearizing the renormalization equations at the fixed points and calculating the eigenvalues. The linearized relation of the renormalization equations is given by

$$\begin{bmatrix} \delta\sigma' \\ \delta\sigma_\eta \end{bmatrix} = \begin{bmatrix} \frac{\partial R_1}{\partial\sigma} & \frac{\partial R_1}{\partial\sigma_\eta} \\ \frac{\partial R_\eta}{\partial\sigma} & \frac{\partial R_\eta}{\partial\sigma_\eta} \end{bmatrix}_{\rm DLA} \begin{bmatrix} \delta\sigma \\ \delta\sigma_\eta \end{bmatrix} \quad \text{for } \eta<1 , \tag{23}$$

$$\begin{bmatrix} \delta\sigma' \\ \delta(1/\sigma_\eta)' \end{bmatrix} = \begin{bmatrix} \frac{\partial R_1}{\partial\sigma} & \frac{\partial R_1}{\partial(1/\sigma_\eta)} \\ \frac{\partial R_\eta}{\partial\sigma} & \frac{\partial R_\eta}{\partial(1/\sigma_\eta)} \end{bmatrix}_{\eta} \begin{bmatrix} \delta\sigma \\ \delta(1/\sigma_\eta) \end{bmatrix}$$

$$\text{for } \eta>1 . \tag{24}$$

Here the matrix is evaluated at the DLA point for $\eta<1$ and at the η point for $\eta>1$. The values of the matrix elements are numerically calculated from the renormalization functions (20) and (21). We obtain the crossover exponents $\phi=0.79$ $(\eta=0.2)$, $\phi=0.86$ $(\eta=2)$, and $\phi=2.39$ $(\eta=4)$. The exponent ϕ is dependent upon the parameter η.

IV. THERMODYNAMIC REPRESENTATION OF THE CROSSOVER

In Secs. II and III we find that if $\eta<1$, the crossover from the DLA fractal to the dense η fractal occurs, and if $\eta>1$ the inverse crossover from the lean η fractal to the DLA fractal appears. The crossover radius between the DLA fractal and the η fractal is controlled by changing the applied voltage. We try to formulate the crossover in terms of a thermodynamic representation of two-phase equilibrium. We define, respectively, the DLA fractal and the η fractal as the DLA phase and the η phase. The pattern showing the crossover between the DLA fractal and the η fractal is presumed to be in a equilibrium state of the two phases. We define the volume fraction x by the crossover radius

$$x=(L^d-r_c^d)/L^d=1-(r_c/L)^d , \tag{25}$$

where L is the size of the pattern and d the dimension of space. When $\eta<1$, the volume fraction x gives the ratio of the volume of the DLA fractal to the total volume of the pattern. With increasing the applied voltage, the volume fraction x increases. The part of the DLA fractal increases. Following to the thermodynamic formalism for the multifractal of the growth probability distribution,[22,23] the spectrum $\tau(q)=(q-1)D(q)$ of moments describing the growth probability distribution is interpreted as the free energy. The order q of the moment is interpreted as the inverse $(1/T)$ of temperature. In general, the thermodynamic potential in an equilibrium state of two phases is given by the sum of the two potentials multiplied by the volume fraction of each phase. Thus the spectrum of the pattern is given by

$$(q-1)D(q)=\begin{cases} x(q-1)D_1(q)+(1-x)(q-1)D_\eta(q) & \text{for } \eta<1 \\ x(q-1)D_\eta(q)+(1-x)(q-1)D_1(q) & \text{for } \eta>1 \end{cases} \tag{26}$$

where $D_1(q)$ and $D_\eta(q)$ indicate, respectively, the generalized dimensions of the DLA fractal and the η fractal. Figure 7 shows the diagram of $D(q)$ against q^{-1} schematically. The diagrams (a) and (b) indicate the cases of $\eta<1$ and $\eta>1$. The two curves in each figure show the saturation line of each phase. The pattern showing the crossover is interpreted as a thermodynamic equilibrium state of two phases. The internal energy α and the entropy f of the pattern are also given by the sum of the two phases

$$\begin{aligned} &\alpha=x\alpha_1+(1-x)\alpha_\eta, \quad f=xf_1+(1-x)f_\eta \quad \text{for } \eta<1 , \\ &\alpha=x\alpha_\eta+(1-x)\alpha_1, \quad f=xf_\eta+(1-x)f_1 \quad \text{for } \eta>1 , \end{aligned} \tag{27}$$

where α_1 and α_η are the internal energies of the DLA fractal and the η fractal, and f_1 and f_η are the entropies of the DLA fractal and the η fractal. Thus we can obtain the generalized dimension $D(q)$ and the α-f spectrum of the pattern showing the crossover by interpreting the crossover pattern as the thermodynamic equilibrium state of two phases.

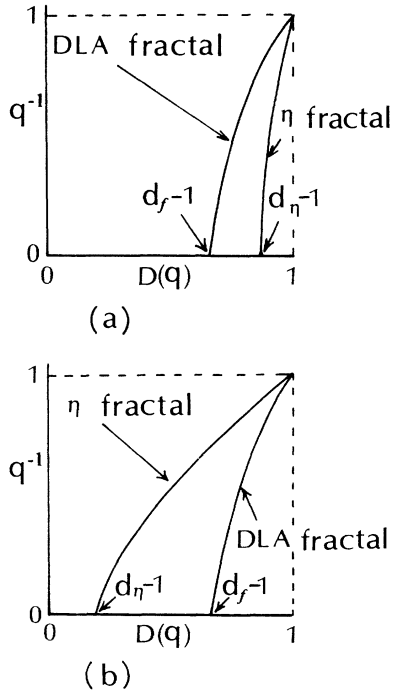

FIG. 7. Schematic diagram of $D(q)[E_f/(q-1)]$ where E_f represents the free energy, against q^{-1} (the temperature). (a) $\eta<1$, (b) $\eta>1$. The pattern showing the crossover is interpreted as a thermodynamic equilibrium state of two phases. The region between two curves represents the mixture of the two phases in a equilibrium states.

V. SUMMARY

We propose an extended η model showing crossover phenomena between the DLA fractal and the η fractal. We analyze the crossover phenomena by using the dimensional analysis and the position-space renormalization-group method. We find that when $\eta < 1$ the crossover from the DLA fractal to the η fractal occurs with increasing size, and when $\eta > 1$ the inverse crossover from the η fractal to the DLA fractal appears. We also show that the crossover radius is controlled by changing the applied field. The global flow diagram in the two-parameter space and the crossover exponent are obtained by the renormalization-group method. We show that the crossover phenomena can be described in terms of a thermodynamic representation of the two-phase equilibrium.

[1]T. A. Witten and L. M. Sander, Phys. Rev. Lett. **47**, 1400 (1981); Phys. Rev. B **27**, 5686 (1983).
[2]P. Meakin, Phys. Rev. A **27**, 1495 (1983); **27**, 604 (1983); **27**, 2616 (1983).
[3]*Kinetics of Aggregation and Gelation,* edited by F. Family and D. P. Landau (North-Holland, Amsterdam, 1984).
[4]*On Growth and Form,* edited by H. E. Stanley and N. Ostrowsky (Nijhoff, the Hague, 1985).
[5]*Fractals in Physics,* edited by L. Pietronero and E. Tosatti (North-Holland, Amsterdam, 1986).
[6]P. Meakin, in *Phase Transitions and Critical Phenomena,* edited by C. Domb and J. L. Lebowitz (Academic, New York, 1988), Vol. 12, p. 336.
[7]R. Jullien and R. Botet, *Aggregation and Fractal Aggregates* (World-Scientific, Singapore, 1987).
[8]J. Feder, *Fractals* (Plenum, New York, 1988).
[9]*Random Fluctuations and Pattern Growth,* edited by H. E. Stanley and N. Ostrowsky (Kluwer Academic, Dordrecht, 1988).
[10]T. Vicsek, *Fractal Growth Phenomena* (World-Scientific, Singapore, 1989).
[11]L. Niemeyer, L. Pietronero, and H. J. Wiesmann, Phys. Rev. Lett. **52**, 1033 (1984).
[12]L. Pietronero and H. J. Wiesmann, J. Stat. Phys. **36**, 909 (1984).
[13]D. Grier, E. Ben-Jacob, R. Clarke, and L. M. Sander, Phys. Rev. Lett. **56**, 1264 (1986).
[14]R. Lenormand, Physica (Amsterdam) **140A**, 114 (1986).
[15]R. F. Voss, J. Stat. Phys. **36**, 861 (1984).
[16]P. Meakin, Phys. Rev. B **28**, 5221 (1983).
[17]Y. Usami and T. Nagatani, J. Phys. Soc. Jpn. **59**, 474 (1990).
[18]J. Lee, A. Coniglio, and H. E. Stanley, Phys. Rev. A **41**, 4589 (1990).
[19]T. Nagatani, J. Phys. A **20**, L381 (1987); Phys. Rev. A **36**, 5812 (1987); **38**, 2632 (1988).
[20]T. Nagatani, Phys. Rev. A **40**, 7286 (1989).
[21]P. Meakin, Annu. Rev. Phys. Chem. **39**, 237 (1988).
[22]T. C. Halsey, P. Meakin, and I. Procaccia, Phys. Rev. Lett. **56**, 854 (1986).
[23]C. Amitrano, A. Coniglio, and F. di Liberto, Phys. Rev. Lett. **57**, 1016 (1986).